

The effect of dilute nitrogen on nonlinear optical properties of the InGaAsN/GaAs single quantum wells

K. Köksal^{1,a} and M. Şahin²

¹ Physics Department, Faculty of Arts and Science, Bitlis Eren University, 13000 Bitlis, Turkey

² Department of Material Science and Nanotechnology Engineering, Abdullah Gül University, Aşık Veysel Bulvarı, Erciyes Teknopark, No: 4/67-A, 38039 Melikgazi, Kayseri, Turkey

Received 2 July 2012 / Received in final form 15 August 2012

Published online 26 September 2012 – © EDP Sciences, Società Italiana di Fisica, Springer-Verlag 2012

Abstract. In this study, we investigate the linear and third order nonlinear optical properties of InGaAsN/GaAs depending on nitrogen content and laser dressing parameter. As theoretical models, band anticrossing and model solid theory are used. In order to obtain the electronic properties of the quantum well, the finite difference method is used. The laser beam affects the electronic properties of the quantum well by changing the shape of the confinement potential. This modification of the potential is determined by laser dressing parameter. By using dilute amount of nitrogen, conduction band and the depth of quantum well can be controlled. The strain which is introduced due to the presence of nitrogen can be compensated by using indium atoms. The electronic and the linear and third order nonlinear optical properties of InGaAsN/GaAs quantum well structure are obtained.

1 Introduction

InGaAsN on GaAs substrate is a very promising material on account of its technological applications [1–5]. Although nitrogen incorporated III-V zincblende semiconductors have been studied for a long time, there are still some mysterious and hidden points about the effect of the nitrogen on its structural, electronic and optical properties [6–9]. According to experimental and theoretical points of view, incorporation of nitrogen into GaAs or III-V semiconductors brings unusual and amazing physical features which can not be obtained by incorporation of different elements. In dilute nitrogen semiconductors, one of the most amazing features is band gap reduction. In usual case, the band gap of a ternary alloy like GaAsN is expected to be placed between those of GaAs and GaN (virtual crystal approximation). However, the band gap of GaAsN tends to have lower values than that of GaAs and very little amount of nitrogen causes huge reduction of the band gap [10]. The most important reason of this unusual feature is explained by high electronegativity of the nitrogen. In order to compensate the strain between GaAsN and GaAs layers and for an additional modification of band gap, In can be introduced to the system [11,12]. Therefore InGaAsN on GaAs is a very promising quantum well (QW) material to obtain 1.3 μm wavelength lasers and photodetectors.

Nitrogen behaves like an impurity and results in a constant energy level in the conduction band (CB) of (In)GaAs. This nitrogen energy level splits the CB into

two subbands. Minimum point of the CB is defined by lowering one of these subbands. The level of the lower conduction subband is very sensitive to the amount of nitrogen incorporation [13]. It is said that only 1% of N (nitrogen) causes a reduction of 150 meV in the band gap of GaAs [14]. The InGaAsN/GaAs QWs can be used as photodetectors because of its high efficient electron confinement. Even at high temperatures, electron can be strongly confined in the well region of the system. In this kind of device, one of the important phenomena is the intersubband transitions. Although there are some experimental and theoretical studies on the intersubband transitions in InGaAsN/GaAs QWs under normal [15,16] and intense [17] laser field, none of them mentioned nonlinear optical properties of this system.

The linear and nonlinear optical properties of the low dimensional semiconductors have received great attention [18–21], with the advances in the laser technology. Nowadays, it is possible to produce high-quality laser beams with high intensity and high frequency. If the intensity and frequency of the laser beam is sufficiently high, it can affect the shape of the quantum well and change its electronic structure. This modification of quantum well leads to a change in linear optical properties of the system. With an additional laser beam source which has a low frequency being resonant to the intersubband transition energy, it is possible to probe the nonlinear optical properties of the quantum well system, which is modified by the high frequency and intensity laser beam.

With this study, we aim to reveal the variation of linear and third order nonlinear optical properties of

^a e-mail: koraykoksal@yahoo.com

InGaAsN/GaAs due to intersubband transitions in conduction band as a function of nitrogen concentration, laser dressing parameter and light intensity. In this study, we assume that the strong laser field affects the shape of the electronic potential as mentioned in the work of Lima et al. [22]. The energy eigenvalues and the corresponding wave functions are calculated by solving the Schrödinger's equation with this modified electronic potential by laser field. The depth of the electronic potential is defined by the amount of Nitrogen concentration and Indium atoms inside the InGaAsN active material.

2 Theory

2.1 Band anti-crossing model

The band anti-crossing (BAC) model, which is firstly offered by Perkins et al. [23], is a very useful technique to reveal the interaction between CB minima of III-V semiconductor and a highly localized energy level due to the impurity like nitrogen. Nowadays, this method has been applied to the semiconductors like GaAsBi because Bi has a strong effect on the valence band (VB) maxima of GaAs and it causes a splitting of valence band into two non-parabolic subbands [7]. As a result of the BAC model for CB, the low energy edges can be given by [24]

$$E_{\pm} = \frac{E_N + E_M \pm \sqrt{(E_N - E_M)^2 + 4V_{MN}^2}}{2} \quad (1)$$

where E_M , E_N are the extended state and N induced energy levels. These levels are relative to the maximum point of the VB. V_{MN} describes an interaction between the localized and the extended states. The mentioned parameters for InGaAsN semiconductor are as following

$$\begin{aligned} E_N &= 1.52 \text{ eV} - y \times 3.9 \text{ eV}, \\ E_M &= E_0 - 1.55 \text{ eV} + \frac{\hbar^2 k^2}{2m_M}, \\ V_{MN} &= \sqrt{y} \times 2.3 \text{ eV}, \end{aligned} \quad (2)$$

where y denotes the nitrogen concentration, E_0 is the CB minima of the InGaAs without N contribution, m_M is the effective mass of InGaAs. These parameters and their dependencies are obtained from experimental results [25]. In order to obtain the electron effective mass in InGaAsN, one has to calculate k -dependent energy by using equation (1). From second derivative of the dispersion (Eq. (1)), effective mass of the lowest conduction band can be found as [26]

$$m^* = \frac{\hbar^2}{\partial_k^2 E_-(k)}. \quad (3)$$

In Figure 1, $E - k$ diagram and nitrogen dependence of the effective mass can be seen for $N = 0.01$.

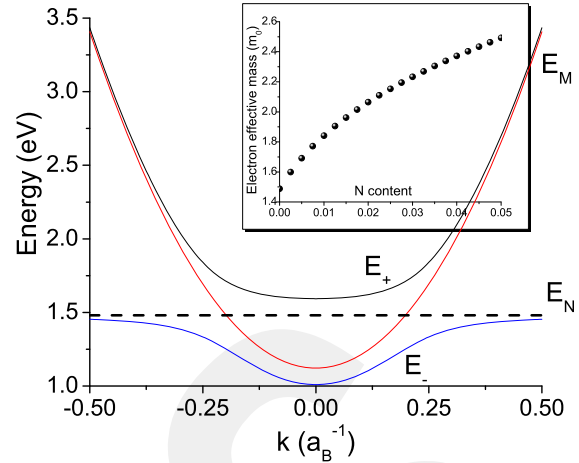


Fig. 1. (Color online) $\text{In}_{0.3}\text{Ga}_{0.7}\text{As}_{0.99}\text{N}_{0.01}$ band structure as a function of wavevector k (in the unit of Bohr radius). Inset figure shows the change of effective mass with the nitrogen concentration. Here E_N (dashed line), E_M (red line) indicate the N induced energy levels and the extended state, respectively. E_{\pm} (blue and black lines) shows the splitted energy bands.

2.2 Model solid theory and the depth of QW

The model solid theory is a technique to calculate the band alignment of the band edges between quantum well and barrier layers [27]. The factors which determine the band alignment are mismatch strain at the interface between layers, bulk band gap energies and spin-orbit split-off band energy, Δ_0 . The strain in a QW system can be calculated as

$$\varepsilon = \frac{a_s - a_e}{a_e} \quad (4)$$

where a_s and a_e are the lattice constants of substrate and epitaxial layer. In order to obtain the valence band position, one needs to know spin split-off band parameter Δ_0 , the change in heavy hole band δE_{hh} due to the strain and the average valence subband energy $E_{v,av}$. If the heavy hole subband is upper than that of the light hole which means the system has compressive strain, the valence band position is

$$E_v(x, y) = E_{v,av}(x, y) + \frac{\Delta_0(x, y)}{3} + \delta E_{hh}(x, y) \quad (5)$$

where x and y denote In (indium) and N contents. If the light hole subband is upper than that of the heavy hole, one also needs to know the change in light hole band δE_{lh} due to the strain. Then the VB position is

$$E_v(x, y) = E_{v,av}(x, y) + \frac{\Delta_0(x, y)}{3} + \delta E_{lh}(x, y) \quad (6)$$

which is used in the case of a tensile strain. The parameters δE_{hh} and δE_{lh} which indicate the shift in heavyhole and lighthole subbands of VB due to the strain are calculated by using some constants like the hydrostatic and

shear deformation potentials and the elastic stiffness constants. δE_{hh} and δE_{lh} can be expressed by

$$\begin{aligned}\delta E_{hh}(x, y) &= 2a_v \left(1 - \frac{C_{12}}{C_{11}}\right) \varepsilon + b \left(1 + \frac{2C_{12}}{C_{11}}\right) \varepsilon, \\ \delta E_{lh}(x, y) &= 2a_v \left(1 - \frac{C_{12}}{C_{11}}\right) \varepsilon - b \left(1 + \frac{2C_{12}}{C_{11}}\right) \varepsilon,\end{aligned}\quad (7)$$

where a_v is the VB hydrostatic deformation potentials, b is the VB shear deformation potential, C_{11} and C_{12} are the elastic stiffness constants.

In order to calculate the conduction position, the strained valence band position which is given by equations (5) and (6), the strained band gap E_g , δE_c , δE_{hh} and δE_{lh} should be known. In the case of compressive strain, the CB position can be written as

$$E_c(x, y) = E_v(x, y) + E_g(x, y) + \delta E_c(x, y) - \delta E_{hh}(x, y) \quad (8)$$

and in the case of tensile strain, $E_c(x, y)$ is

$$E_c(x, y) = E_v(x, y) + E_g(x, y) + \delta E_c(x, y) - \delta E_{lh}(x, y) \quad (9)$$

where the shift in CB due to the strain can be calculated by using CB hydrostatic deformation potentials and elastic stiffness constants as

$$\delta E_c(x, y) = 2a_c \left(1 - \frac{C_{12}}{C_{11}}\right) \varepsilon. \quad (10)$$

Therefore, with the help of equations (8), (9), (6), (5) the CB and VB offsets read

$$\begin{aligned}\frac{\Delta E_c}{\Delta E_g} &= \frac{E_c^w - E_c^b}{E_g^b - E_g^w}, \\ \frac{\Delta E_v}{\Delta E_g} &= \frac{E_v^w - E_v^b}{E_g^b - E_g^w},\end{aligned}\quad (11)$$

where the subscripts w and b indicate the well and barriers. E_g^b and E_g^w are the band gaps of barrier and well, respectively. By using the information about the CB offset, it is possible to find out the electronic structure of the QW material.

Because we are dealing with the intersubband transitions in our calculations, the eigenvalues and eigenfunctions of the electrons in conduction band obtained from the Schrödinger's equation with the potential ΔE_c which procedure is explained in the next section.

2.3 Shape of the potential under high intense laser field

An electron which is confined in a square shape finite well with depth which is defined by the difference between the bandgaps of well and barrier materials in quantum well structure is also affected by an applied laser radiation field. In order to obtain dynamical behavior of the electron, time dependent Schrödinger's equation can be written as

$$\left(\frac{[\mathbf{p} + e\mathbf{A}]^2}{2m^*} + V(\mathbf{r})\right) \psi(\mathbf{r}, t) = i\hbar \frac{\partial \psi(\mathbf{r}, t)}{\partial t}, \quad (12)$$

where \mathbf{p} and \mathbf{A} are momentum operator and vector potential due to electromagnetic radiation, respectively. $V(\mathbf{r})$ is time-independent structure potential. The parameters, e , m^* , t , \mathbf{r} are electron charge, electron effective mass, time and position vector, respectively. In this equation

$$\mathbf{A}(t) = \mathbf{u}A_0 \cos(\omega_R t), \quad (13)$$

where \mathbf{u} indicates the unit vector of the polarization. A_0 is the amplitude of the laser beam and ω_R is the frequency of the laser radiation. The square of A_0 gives the laser beam intensity. In order to solve the equation, Coulomb gauge is considered ($\nabla \cdot \mathbf{A} = 0$) [28]. Equation (12) can be transformed to another form as [29]

$$\begin{aligned}\left(-\frac{\hbar^2}{2m^*} \nabla^2 + V(\mathbf{r} + \boldsymbol{\alpha}(t))\right) \psi(\mathbf{r}, t) &= i\hbar \frac{\partial \psi(\mathbf{r}, t)}{\partial t}, \\ \boldsymbol{\alpha}(t) &= \mathbf{u}\alpha_0 \cos(\omega_R t),\end{aligned}\quad (14)$$

where $\alpha_0 = eA_0/(m\omega_R)$ which indicates laser dressing parameter. The physical meaning of this parameter is related to the classical free-electron quiver motion [30,31]. ω_R is the frequency of the laser radiation which is represented by a monochromatic plane wave [32]. Here one can use the Floquet approach to reduce the system into the time-independent Schrödinger's equation [19,33,34]. In our case, the laser field is polarized in growth direction of semiconductor (in z direction).

The confinement potential of the quantum well structure can be written as [22]

$$V(z, N, In) = \Delta E_c(N, In) \Theta(|z| - L_w/2), \quad (15)$$

where L_w is the quantum well width, z is growth direction and Θ is unit step function. In the presence of the external laser field, the shape of the quantum well is changed as [22,32]

$$\begin{aligned}V(z, N, In; \alpha_0) &= \frac{\Delta E_c}{\pi} \Theta\left(\alpha_0 - z - \frac{L_w}{2}\right) \\ &\times \cos^{-1}\left(\frac{L/2 + z}{\alpha_0}\right) \\ &+ \frac{\Delta E_c}{\pi} \Theta\left(\alpha_0 + z - \frac{L_w}{2}\right) \\ &\times \cos^{-1}\left(\frac{L/2 - z}{\alpha_0}\right).\end{aligned}\quad (16)$$

The subband energies and wavefunctions are calculated by solving the Schrödinger's equation

$$\begin{aligned}\frac{\hbar^2}{2m^*} \nabla^2 \psi(z, N, In; \alpha_0) + V(z, N, In; \alpha_0) \psi(z, N, In; \alpha_0) &= \\ E(N, In; \alpha_0) \psi(z, N, In; \alpha_0),\end{aligned}\quad (17)$$

where effective mass of electron can be considered having a linear dependency on nitrogen content as calculated by

Lindsay and O'Reilly [35]. But, the best way is to obtain it from $E - k$ diagram of the conduction band. The electron effective mass for $\text{Ga}_{0.7}\text{In}_{0.3}\text{As}$ which can be found by using interpolation between the GaAs and InAs parameters is $0.054m_0$. In order to obtain nitrogen dependent effective mass we use equation (3).

We assume that the quantum well system under investigation is illuminated by two different laser fields [36] (their frequencies are ω_R and ω) which are polarized along growth direction of the QW. One of the laser fields with ω_R modifies shape of the quantum well potential. The other laser field with ω is used to observe the intersubband transitions between substates in the case of $\omega = (E_j - E_i)/\hbar$ (E_j and E_i are final and initial electron energy values in QW) and related linear and nonlinear optical properties. If the intensity is sufficiently high, a change in the intensity of second laser field (ω) causes nonlinear effects in the quantum well system. α_0 which is a parameter to produce the dressed potential is related to the intensity and frequency ω_R of the first laser field. α_0 , well known term in atomic physics [31], is used to control and manipulate the carrier confined in an atomic potential by modifying the shape of the potential. In atomic physics, the high-intensity field is a nice tool to manipulate the atomic potential as in solid state physics. In this study, 5 different values of α_0 are used to manipulate the subband states by modifying the dressed potential. It should be noted that the case of $\alpha_0 = 0$ indicates that the laser field with ω_R is turned off.

2.4 Absorption coefficients

The absorption coefficients can be calculated by using the wavefunctions and energy eigenvalues. The absorption coefficient can be written as in references [37,38] with some further modifications

$$\alpha(\omega, I) = \alpha^{(1)}(\omega) + \alpha^{(3)}(\omega, I) \quad (18)$$

where $\alpha^{(1)}$ and $\alpha^{(3)}$ are linear and third order nonlinear absorption coefficients which can be expressed by

$$\alpha^{(1)}(\omega) = \omega \sqrt{\frac{\mu}{\varepsilon}} \frac{n\hbar\Gamma_{ij} |M_{ji}|^2}{(E_{ij} - \hbar\omega)^2 + (\hbar\Gamma_{ij})^2},$$

$$\alpha^{(3)}(\omega, I) = -\omega \sqrt{\frac{\mu}{\varepsilon}} \left(\frac{I}{2\varepsilon_0 n_r c} \right) \frac{4n\hbar\Gamma_{ij} |M_{ji}|^4}{((E_{ij} - \hbar\omega)^2 + (\hbar\Gamma_{ij})^2)^2},$$

where i, j denote the initial and final states, E_i (E_j) initial (final) state energy, $E_{ij} = E_j - E_i$, ε and μ are the static dielectric permittivity and permeability of the material, respectively. n is the electron density (we choose $n = 10^{18} \text{ cm}^{-3}$ which is below the amount that can change the value of effective mass [39]), $\hbar\Gamma_{ij}$ is the line width, I is the intensity of the incident laser beam, c is the speed of light, n_r is the refractive index of the medium, and M_{ji} is the transition matrix element between initial and final

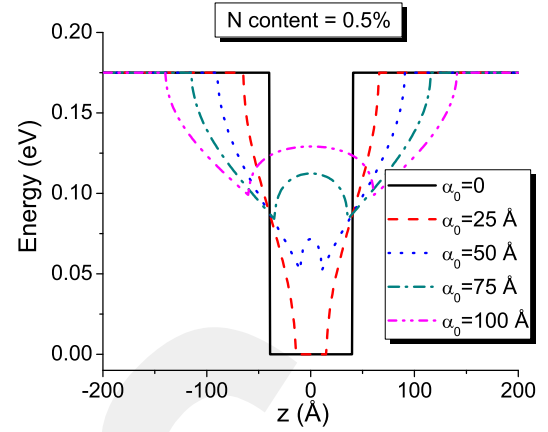


Fig. 2. (Color online) The change of the quantum well shape as a function of dressing parameter α_0 for $N = 0.5\%$.

states. $n, \Gamma_{ij}, I, M_{ji}$ can be formulated as following

$$\Gamma_{ij} = 1/T_{ij},$$

$$I = \frac{2n_r}{\mu c} |E(\omega)|^2,$$

$$M_{ji} = |\langle \psi_j | e z | \psi_i \rangle|,$$

where T_{ij} is the relaxation time, $E(\omega)$ is incident radiation field in z direction. $\psi_{j,i}$ is the wavefunction of an electron which is confined in QW potential which is given by equation (17).

In this point, we have to stress that the intensity, I in $\alpha^{(3)}(\omega, I)$ equation is not dependent on dressing parameter α_0 . Because, we assume that during the experimental procedure, two different laser sources are used: while first one has high intensity and high frequency, second one has low frequency. As well known, photon-photon interaction is omitted in any case.

3 The results and discussions

In our QW system, as mentioned before, GaAs is used as substrate and barrier materials and InGaAsN is used as a well material. In order to observe the effect of the nitrogen contribution on optical properties, the amount of In content is fixed at 30%. The dielectric constant is taken as $\varepsilon = 13.46$ for In = 0.3. The permeability is $\mu = 4\pi \times 10^{-7} \text{ N/A}^2$, the refractive index $n_r = 3.15$ and the relaxation time $T_{ij} = 0.2 \text{ ps}$. The CB values of InGaAsN/GaAs QW is obtained by using the model solid theory and band anticrossing technique. All necessary material parameters are taken from the previous studies [40,41].

Figure 2 shows the variation of confinement potential as a function of the laser dressing parameter, α_0 . As seen from Figure 2, in the case of In = 30%, $N = 0.5\%$, $L_w = 80 \text{ Å}$, the shape of the QW can be drastically changed by α_0 of the applied laser beam which is linearly

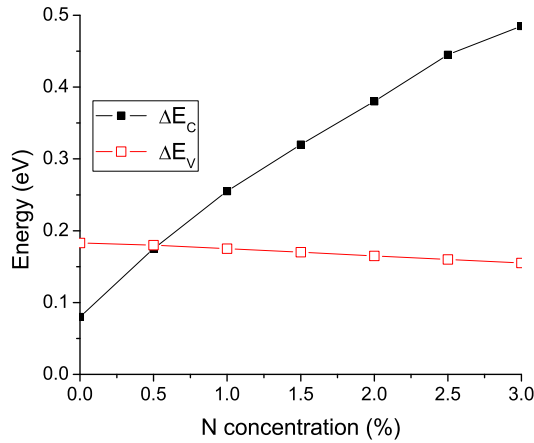


Fig. 3. (Color online) For $\text{In} = 30\%$, the change of the conduction and valence band offsets with increasing nitrogen concentration.

polarized in z direction. The change in the shape is obtained by equation (16). α_0 is related to the strength of the laser beam and it has a strong effect on the shape of the QW. α_0 can be used as a tuning parameter to control the shape of the QW. The effect of the laser beam has been investigated in different reported studies [22,32]. They have used time dependent perturbation theory to reveal the change of the well under an applied electromagnetic radiation which is polarized in the growth direction of QW.

The conduction band offset is strongly dependent on the amount of N concentration. As mentioned in the literature [42], nitrogen is an unusual component for III-V semiconductors because it causes reductions of band gap and lattice constant at the same time. However, in a usual case, band gap values are inversely proportional to the lattice constants. This is a great advantage for band gap engineering to broad the range of laser and detector applications. Figure 3 shows the variation of valance and conduction band offset with nitrogen. As can be seen from the figure, for $\text{In} = 30\%$ the CB offset is increasing with the increase in N concentration. The addition of 3% N causes an increase of 400 meV in the conduction band offset. The change in VB offset is not so much and hole is trapped in shallow quantum wells. However, even in shallow VB quantum wells, hole is well confined because its mass is much heavier than that of CB electron. In Figure 3, the most remarkable point is that deep CB offset leads to a better confinement of conduction electrons in QW and high efficiency in high temperatures.

In Figure 4, the change of first and second electron state energies is shown as a function of α_0 and nitrogen content. Introduction of N to the system leads to an increase in the depth of the quantum well and a separation between electron energy levels. While deeper QW results in a small increase in the first state energy, it causes relatively larger increase in the second state energy. The figure shows that an increase in α_0 reduces the difference between first and second energy levels of the electron. This situation can be explained by the fact that the potential

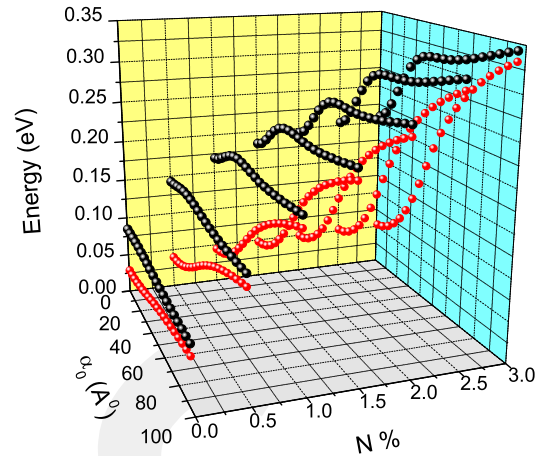


Fig. 4. (Color online) The variation of the first and second electron state energies with the change of nitrogen concentration and dressing parameter α_0 . We assume that In concentration and well width are 30% and 80 Å, respectively.

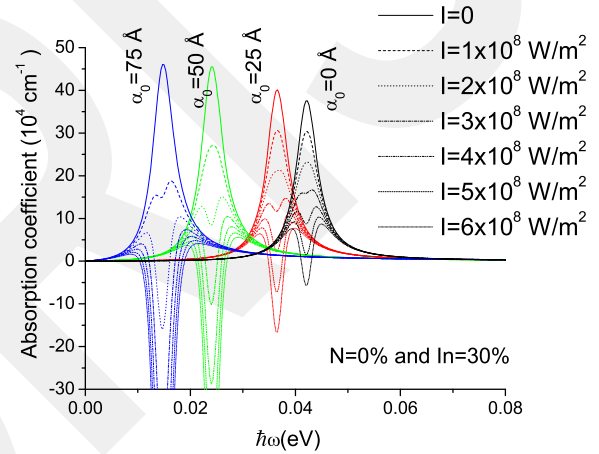


Fig. 5. (Color online) The change in absorption coefficient as a function of incoming photon energy in the case of $N = 0\%$. Every color indicates a different laser dressing parameter (0, 25, 50 and 75 Å). The change of line style shows the change in the intensity of the laser beam. The negative absorption coefficient values can be interpreted as numerical artefact.

shape changes from a deep square well to a shallow broad well as seen in Figure 2. In addition, an increase in both α_0 and N content causes increasing energy levels. For the highest values of α_0 and N content, this increment is so large for first electron state that makes the both electron states have nearly the same energy, which is the highest value in entire spectrum.

The understanding of optical properties of QWs is very important for device application. As can be seen from equation (19), although the linear absorption coefficient does not depend on the absorbing light intensity, the third order absorption one (also total absorption one) is linearly proportional to the light intensity. The linear and total absorption coefficients depending on intense laser field effect and absorbing light intensity are plotted in Figure 5 for $\text{In}_{0.3}\text{Ga}_{0.7}\text{As}/\text{GaAs}$ QW system. The effects of the laser dressing parameter α_0 and the intensity of absorbing laser

photon on the absorption coefficients are evidently seen from the figure, because N is not included in this system. Although the linear absorption coefficient, corresponding to $I = 0$, is not depending on the light intensity, it increases with increasing α_0 . In addition, we can predict from the total absorption coefficient that the intense laser field drastically affects the third order nonlinear absorption coefficients. For example, when $I = 1 \times 10^8 \text{ W/m}^2$, while there is no bleaching effect on the total absorption coefficient for $\alpha_0 = 0$ and 25 \AA , it is seen that there is a saturation for $\alpha_0 = 50 \text{ \AA}$ and very high bleaching for $\alpha_0 = 75 \text{ \AA}$. This behavior can be explained by the fact that the wave functions of first and second levels overlap. That means, an increase in the intense laser field results in the overlapping and consequently makes the dipole matrix element larger and causes that the third order absorption coefficients are also increasing. When we focus on the absorption peak position, we see that the absorption peaks shift to small energy values with increasing laser intense field. This is a result of reduction in difference between first and second electron state energies as seen in Figure 4. In this case, the intersubband absorption energy can be tuned by changing the α_0 which is related to the strength of the electromagnetic beam. In addition, the increase in α_0 causes increasing magnitude of $\alpha(\omega, I)$. In order to tune the magnitude of the $\alpha(\omega, I)$, the intensity of the laser should be changed. A decrease in intensity results in a decrease in $\alpha(\omega, I)$. With the increasing intensity, a bleaching begins to be observed and the strength of this bleaching increases.

The electronic properties are very sensitive to the nitrogen content of the structure as seen in Figure 4. Hence, we expect that the optical properties are also very sensitive to N content. In Figure 6, we plot the total absorption coefficients as a function of absorbing photon energy depending on N content and dressing parameters for different light intensity. In Figure 6, the amount of change in light intensity is same with that in Figure 5. By introduction of a little amount of N like 0.5%, the electronic and related optical properties of $\text{In}_{0.3}\text{Ga}_{0.7}\text{As}_{0.995}\text{N}_{0.005}/\text{GaAs}$ QW system is drastically changed as seen in Figure 6a. When we compared the cases 0% with 0.5%, it can be seen that all the absorption peaks are positioned at higher energy values (blue shift) in latter case. From Figures 6a–6d, it is possible to observe that the absorption peaks are shifting to higher energy values with increasing N content. If we take a closer look at these changes in Figure 6, we see that peak positions of $\alpha_0 = 25$ and $\alpha_0 = 50 \text{ \AA}$ change while that of $\alpha_0 = 75 \text{ \AA}$ remains almost unchanged. The shift in peak position of $\alpha_0 = 0 \text{ \AA}$ is less than those of $\alpha_0 = 25$ and $\alpha_0 = 50 \text{ \AA}$. When the nitrogen content is increased to 1%, $\alpha_0 = 0$ and $\alpha_0 = 25$ peaks completely overlaps and they are found at 0.09 eV. This can be explained by the fact that N causes a smaller band gap and a deeper conduction band well. When electrons feel more confinement in a deeper well, the difference between their energies increases as seen in Figure 4. One needs to notice that the most important effect of N is seen at $\alpha_0 = 0$ and $\alpha_0 = 25 \text{ \AA}$.

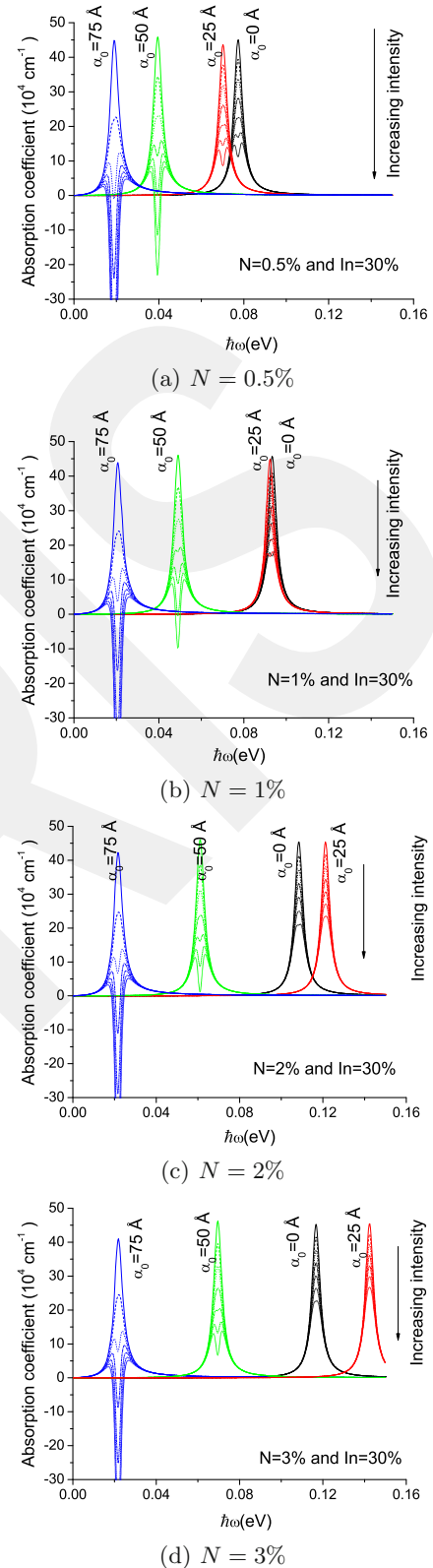


Fig. 6. (Color online) The change in absorption coefficient as a function of incoming photon energy in the case of $N = 0.5\%$ (a), $N = 1\%$ (b) and $N = 2\%$ (c) and $N = 3\%$ (d). Every color indicates a different laser dressing parameter (0, 25, 50, 75 Å). The change of line style shows the change in the intensity of the laser beam.

The linear absorption peaks are not dramatically affected from the content of N . In contrast to this, the N content is to be effective on decreasing tendency of the nonlinear optical coefficients. For example, for $\alpha_0 = 50 \text{ \AA}$, while the bleaching is observed at $I = 3 \times 10^8 \text{ W/m}^2$ for $N = 0.5\%$ and 1.0% , it is seen at $I = 4 \times 10^8 \text{ W/m}^2$ for $N = 2.0\%$ and 3.0% .

The effect of nitrogen, intensity and dressing parameter can be seen clearly in Figure 6b. With the increase of laser intensity, bleaching begins to be observed. The strength of the bleaching in $\alpha_0 = 50$ and $\alpha_0 = 75$ cases is stronger than that in $\alpha_0 = 0$ and $\alpha_0 = 25$ cases, which means that an increase in α_0 does not affect only the position of absorption peaks, but also the strength of bleaching. From Figure 6b, we can conclude that nitrogen tends to eliminate the effect of the dressing parameter.

When nitrogen content is increased to 2%, as can be seen from Figure 6c, $\alpha_0 = 0$ peak is placed at lower frequency compared with that of $\alpha_0 = 25 \text{ \AA}$ peak. It shows that the dressing parameter does not have always a red shifting effect. Sometimes, a deeper well due to the nitrogen content can eliminate this effect. From Figures 6c and 6d, we can also conclude that if $N > 2\%$ and $0 < \alpha_0 < 25 \text{ \AA}$, α_0 leads to a decrease in position of absorption coefficient peaks. For peaks corresponding to the values $\alpha_0 = 25$ and $\alpha_0 = 0 \text{ \AA}$, it is very hard to observe the bleaching for given intensity range which means that the effect of intensity becomes less with increasing nitrogen.

In Figure 6d, when nitrogen content is increased to 3%, $\alpha_0 = 0 \text{ \AA}$ and $\alpha_0 = 25 \text{ \AA}$ peaks are placed at 0.12 eV and at 0.15 eV, respectively. The differences between the peak positions are bigger than those in the previous figures.

In Figures 5 and 6, one has to notice that the negative absorption coefficient appears for high intensity in some cases. In our opinion this is an artefact because of theoretical approach which is described in equation (18). As well known, the validity of the perturbation is limited by the intensity of light

In our calculations, the reason of keeping indium content as a constant is to clearly indicate the effect of nitrogen on the electronic and optical properties. Indium does not have a great influence on the depth of quantum well, but it is a tool to modify and balance the strain of the system. The effect of indium on nonlinear optical properties can be shown in future.

4 The conclusion

We investigated the variation of electronic properties in InGaAsN/GaAs QW system with the change of nitrogen content and laser dressing parameter. We showed that nitrogen and dressing parameters have different kind of effects on the energy levels of subband electrons [43,44]. Nitrogen incorporation gives a rise an increment of the eigenvalues. When $N < 2\%$, an increase in dressing parameter makes first electron energy higher and second one lower. If $N > 2\%$, the dressing parameter will raise the energy values of both electron states. This change of the

electronic structure results in important modifications of optical properties of the system. We also investigated that the change of linear absorption coefficient ($I = 0$) for different nitrogen contents and dressing parameters. The results revealed that nitrogen has a red shifting effect on the linear absorption coefficients. Amount of shifting also depends on the dressing parameter so that while the shifting is nearly negligible for large values of the dressing, it is very significant for small values. Up to our knowledge, as a first time, we showed the effect of applied high-intense laser field on the nonlinear absorption coefficient of InGaAsN/GaAs single QW system. Increasing intensity has no influence on the position of absorption peaks. However, the intensity causes a bleaching effect on the nonlinear absorption coefficient and the nitrogen provides an opposite effect and reduces the bleaching. Nitrogen tends to eliminate the effect of dressing parameters, it decreases the bleaching and compensates the red shift of frequency. We also observed that an increase in the dressing parameter results in a very strong bleaching effect, which is not possible to observe in other situations. We believe that dilute nitrogen semiconductor can be very talent candidate to be used as a quantum well material under intense laser field. And it is possible to control the linear and nonlinear optical properties of the material by tuning laser parameters and nitrogen content.

K.K. wish to thank the TUBITAK for financial support during this study.

References

1. R. Carron, D. Fekete, P. Gallo, B. Dwir, A. Rudra, M. Felici, B. Bartova, M. Cantoni, E. Kapon, Appl. Phys. Lett. **99**, 101107 (2011)
2. R. Carron, P. Gallo, B. Dwir, A. Rudra, E. Kapon, Appl. Phys. Lett. **99**, 181113 (2011)
3. D. Fekete, R. Carron, P. Gallo, B. Dwir, A. Rudra, E. Kapon, Appl. Phys. Lett. **99**, 072116 (2011)
4. M.J. Milla, A. Guzmán, R. Gargallo-Caballero, J.M. Ulloa, A. Hierro, J. Cryst. Growth **324**, 215 (2011)
5. W. Tzung-Han, S. Yan-Kuin, L. Yi-Chieh, W. Yu-Jen, Jpn J. Appl. Phys. **50**, 01AD07 (2011)
6. M. Seifkar, E.P. O'Reilly, S. Fahy, Phys. Rev. B **84**, 165216 (2011)
7. J. Hwang, J.D. Phillips, Phys. Rev. B **83**, 195327 (2011)
8. V.M. Mikoushkin, Appl. Surf. Sci. **257**, 4941 (2011)
9. M.C. Hsieh, J.F. Wang, Y.S. Wang, C.H. Yang, R.C.C. Chen, C.H. Chiang, Y.F. Chen, J.F. Chen, J. Appl. Phys. **110**, 103709 (2011)
10. H. Baaziz, Z. Charifi, A. Reshak, B. Hamad, Y. Al-Douri, Applied Physics A: Materials Science and Processing **106**, 687 (2012)
11. K. Köksal, B. Gönül, M. Oduncuoğlu, Eur. Phys. J. B – Condens. Matter Complex Systems **69**, 211 (2009)
12. P. Chang, E.S.E. Division, E.S. Meeting, *State-of-the-Art Program on Compound Semiconductors XXXVII (SOTAPOCS XXXVII) and Narrow Bandgap Optoelectronic Materials and Devices: Proceedings of the International Symposia, Proceedings* (Electrochemical Society) (Electrochemical Society, 2002), ISBN 9781566773362

13. J. Buckeridge, S. Fahy, Phys. Rev. B **84**, 144120 (2011)
14. J.Y. Duboz, J.A. Gupta, Z.R. Wasilewski, J. Ramsey, R.L. Williams, G.C. Aers, B.J. Riel, G.I. Sproule, Phys. Rev. B **66**, 085313 (2002)
15. H.C. Liu, C.Y. Song, J.A. Gupta, G.C. Aers, Appl. Phys. Lett. **89**, 241122 (2006)
16. J.Y. Duboz, M. Hugues, B. Damilano, A. Nedelcu, P. Bois, N. Kheirodin, F.H. Julien, Appl. Phys. Lett. **94**, 022103 (2009)
17. F. Urgan, E. Kasapoğlu, C. Duque, H. Sarı, I. Sökmen, Physica E: Low-dimens. Syst. Nanostruct. **44**, 515 (2011)
18. L. Lu, W. Xie, H. Hassanabadi, J. Lumin. **131**, 2538 (2011)
19. Q. Fanyao, A.L.A. Fonseca, O.A.C. Nunes, Phys. Rev. B **54**, 16405 (1996)
20. H.S. Brandi, A. Latgé, L.E. Oliveira, Phys. Rev. B **70**, 153303 (2004)
21. U. Yesilgül, S. Şakiroğlu, E. Kasapoğlu, H. Sarı, I. Sökmen, Physica B: Condens. Matter **406**, 1441 (2011)
22. F.M.S. Lima, M.A. Amato, O.A.C. Nunes, A.L.A. Fonseca, B.G. Enders, J.E.F. da Silva, J. Appl. Phys. **105**, 123111 (2009)
23. J.D. Perkins, A. Mascarenhas, Y. Zhang, J.F. Geisz, D.J. Friedman, J.M. Olson, S.R. Kurtz, Phys. Rev. Lett. **82**, 3312 (1999)
24. W. Shan, W. Walukiewicz, J.W.A. III, E.E. Haller, J.F. Geisz, D.J. Friedman, J.M. Olson, S.R. Kurtz, J. Appl. Phys. **86**, 2349 (1999)
25. I. Suemune, K. Uesugi, W. Walukiewicz, Appl. Phys. Lett. **77**, 3021 (2000)
26. R.J. Potter, N. Balkan, J. Phys.: Condens. Matter **16**, S3387 (2004)
27. C.G. Van de Walle, Phys. Rev. B **39**, 1871 (1989)
28. F.M.S. Lima, M.A. Amato, L.S.F. Olavo, O.A.C. Nunes, A.L.A. Fonseca, E.F. da Silva, Phys. Rev. B **75**, 073201 (2007)
29. H.A. Kramers, *Collected Scientific Papers*, (North-Holland, Amsterdam, 1956), ISBN 3893194622
30. Q. Fanyao, A. Fonseca, O. Nunes, Superlatt. Microstruct. **23**, 1005 (1998)
31. M. Fedorov, M.V. Fedorov, *Atomic and Free Electrons in a Strong Light Field* (World Scientific, 1997)
32. E.C. Niculescu, L.M. Burileanu, Eur. Phys. J. B **74**, 117 (2010)
33. M. Gavrilă, J.Z. Kamiński, Phys. Rev. Lett. **52**, 613 (1984)
34. M. Pont, N.R. Walet, M. Gavrilă, C.W. McCurdy, Phys. Rev. Lett. **61**, 939 (1988)
35. A. Lindsay, E.P. O'Reilly, Phys. Rev. Lett. **93**, 196402 (2004)
36. S. Şakiroğlu, F. Urgan, U. Yesilgül, M. Mora-Ramos, C. Duque, E. Kasapoğlu, H. Sarı, I. Sökmen, Phys. Lett. A **376**, 1875 (2012)
37. İ. Karabulut, S. Baskoutas, J. Appl. Phys. **103**, 073512 (2008)
38. S. Ünlü, I. Karabulut, H. Şafak, Physica E: Low-dimens. Syst. Nanostruct. **33**, 319 (2006)
39. C. Skierbiszewski, Semicond. Sci. Technol. **17**, 803 (2002)
40. B. Gönül, K. Köksal, E. Bakır, Physica E: Low-dimens. Syst. Nanostruct. **31**, 148 (2006)
41. B. Gönül, E. Bakır, K. Köksal, Semicond. Sci. Technol. **21**, 876 (2006)
42. A. Erol, *Dilute III-V Nitride Semiconductors and Material Systems: Physics and Technology* (Springer series in materials science, Springer, 2008)
43. F. Urgan, E. Kasapoğlu, H. Sarı, I. Sökmen, Eur. Phys. J. B **82**, 313 (2011)
44. E. Kasapoğlu, C. Duque, S. Şakiroğlu, H. Sarı, I. Sökmen, Physica E: Low-dimens. Syst. Nanostruct. **43**, 1427 (2011)